

## Rotational vortex-flux characteristics of a type-II superconductor

H. P. Goeckner and J. S. Kouvel

*Department of Physics, University of Illinois at Chicago, Chicago, Illinois 60680*

(Received 13 January 1994)

The rotation of a superconducting sample in a fixed field  $\mathbf{H}$ , starting in a hysteretic state, is known to produce a bifurcation of the vortex-flux density into a trapped rotational component  $\mathbf{B}_R$ , which turns rigidly with the sample, and a frictional component  $\mathbf{B}_F$ , which stays fixed relative to  $\mathbf{H}$ , reflecting the effects of vortex pinning and unpinning. Our rotational magnetic measurements on polycrystalline  $(\text{Ba,K})\text{BiO}_3$  at 4.2 K now show that both  $B_R$  and  $B_F$  and their changes with  $H$  are the same for starting states on different branches of a major hysteresis loop. Moreover, for starting states after zero-field cooling, we find that  $B_R$  is zero for all  $H$  but that  $B_F$  rises at  $H_{c1}$  and rapidly joins the  $B_F$  values for the hysteretic starting states at higher  $H$ . Hence, regardless of the magnetic history before sample rotation, the frictional component  $B_F$  depends essentially only on  $H$  (at fixed temperature) and thus equilibrates with the magnetic environment.

For intrinsic as well as technological reasons, the pinning of vortex lines in a type-II superconductor continues to be of considerable active interest. Experimentally, via the use of critical-state models,<sup>1-3</sup> the strength of the vortex pinning in various materials has typically been determined from the width of magnetic hysteresis loops<sup>4</sup> and from the time dependence (or creep) of the vortex flux.<sup>5</sup> A more direct alternative method is provided by measurements of the magnetization vector ( $\mathbf{M}$ ) of a sample disk that is rotated about its axis in a fixed magnetic field ( $\mathbf{H}$ ) applied parallel to the plane of the disk. Rotational magnetization-vector (RMV) measurements were originally carried out in our laboratory<sup>6</sup> on polycrystalline Nb and  $\text{YBa}_2\text{Cu}_3\text{O}_7$  samples rotated at 4.2 K in a moderately high  $H$ , and they showed that the magnetic flux density  $\mathbf{B}$  turns by some small angle relative to  $\mathbf{H}$ , where it remains as the sample continues to rotate. Since  $\mathbf{B}$  derives exclusively from the vortex flux,<sup>6</sup> this behavior evidences a frictional torque exerted on the vortices by the rotating sample via a sequential unpinning-repinning process. Moreover, the magnitude and orientation of the frictional  $\mathbf{B}$  were found to be the same for the same  $H$ , independent of the thermomagnetic history of the sample before rotation.

The RMV measurements on the  $\text{YBa}_2\text{Cu}_3\text{O}_7$  sample were subsequently extended to lower fields,<sup>7</sup> where it was observed that the vortex-flux density consists not only of a frictional component  $\mathbf{B}_F$  but also of a component  $\mathbf{B}_R$  that rotates rigidly with the sample and may therefore be regarded as a trapped component. This directional bifurcation of  $\mathbf{B}$  and its variations with  $H$  were shown to be consistent with a distribution in the strength of the vortex pinning forces. However, this latter work was limited to the field-cooled state of the sample, and the two components of the bifurcated  $\mathbf{B}$  were not determined explicitly.

We have recently investigated the RMV properties of a thin polycrystalline disk of  $\text{Ba}_{0.575}\text{K}_{0.425}\text{BiO}_3$  in various magnetic states before rotation. The small magnetic an-

isotropy of this cubic perovskite-structured compound<sup>8</sup> (with  $T_c \approx 30$  K) makes it fairly ideal for this type of study. Our initial RMV measurements<sup>9</sup> on this  $(\text{Ba,K})\text{BiO}_3$  sample at 4.2 K revealed a directional bifurcation of  $\mathbf{B}$  that is qualitatively very similar to that seen earlier in  $\text{YBa}_2\text{Cu}_3\text{O}_7$ . We have proceeded with this RMV study in detail and, as reported in this paper, our results show that  $\mathbf{B}_F$  and  $\mathbf{B}_R$ , the frictional and rotational components of  $\mathbf{B}$ , and their separate dependencies on  $H$  are essentially identical for starting states on different branches of a major hysteresis loop. Moreover, when these results are combined with those obtained after zero-field cooling, they demonstrate that  $B_F$  versus  $H$  (above  $H_{c1}$ ) is totally independent of the starting state of the sample.

For our  $(\text{Ba,K})\text{BiO}_3$  sample at 4.2 K, the magnetization  $M$  versus  $H$  is plotted in Fig. 1(a) and contains the initial zero-field-cooled (ZFC) curve and the central portions of the upper and lower branches (UHB and LHB) of the hysteresis loop obtained by cycling  $H$  between  $\pm 14$  kOe; the demagnetization correction of  $H$  is negligibly small. In Fig. 1(b), the same data have been converted to a plot of flux density  $B (= 4\pi M + H)$  versus  $H$ . As previous rotational experiments have confirmed,<sup>6</sup> this conversion corresponds to a consistent correction of  $M$  for its diamagnetic shielding component ( $-H/4\pi$ ), so that  $B$  represents exclusively the vortex-flux density, whose behavior we have studied upon subsequent sample rotation.

In our rotational experiments, we made use of a cryogenic vibrating-sample magnetometer system with two sets of pickup coils mounted in quadrature,<sup>6</sup> which allowed us to measure simultaneously the components of  $\mathbf{M}$  parallel and perpendicular to the fixed  $\mathbf{H}$  in the plane of the sample disk which is rotated about its axis. The data were then converted to  $B_L$  and  $B_T$ , the longitudinal and transverse components of  $\mathbf{B}$  relative to  $\mathbf{H}$ . In Fig. 2, our results for  $B_L$  and  $B_T$  are plotted against each other

for the sample in UHB and LHB starting states at  $H=0.25$  kOe. The points in these polar plots represent the ends of  $\mathbf{B}$  vectors emanating from the origin, which shift in direction as the sample is rotated clockwise from  $\theta=0$  to  $360^\circ$  and then counterclockwise back to  $\theta=0$  relative to the fixed  $\mathbf{H}$ ; the points are marked at  $\theta$  intervals of  $180^\circ$ . The initial point at  $\theta=0$  is strongly positive in the UHB case and negative in the LHB case, corresponding to the opposite polarities of  $B$  on the two hysteresis-loop branches at this low field [see Fig. 1(b)]. Nevertheless, in the two cases, after an initial transient interval extending up to  $\theta \approx 180^\circ$ , the points begin to fall on circles of nearly equal radius with their centers positioned very similarly. Then, for the reverse sample rotations, again after an initial transient interval, the points describe circles of comparable size but whose centers are located symmetrically on the other side of the  $B_L$  (or  $H$ ) axis.

The circles defined by the polar plots in Fig. 2 show that in the rotational steady state the  $\mathbf{B}$  vector consists of a trapped rotational component  $\mathbf{B}_R$ , whose size equals the circle radius, and a frictional component  $\mathbf{B}_F$ , whose size equals the displacement of the circle center from the origin. What is striking is that  $\mathbf{B}_R$  and  $\mathbf{B}_F$  are each close to the same magnitude for the two different starting states. The fact that  $\mathbf{B}_R$  is opposite in polarity in the two cases presumably reflects the persistence of strongly pinned vortices created near the positive and negative high-field end points of the major loop.

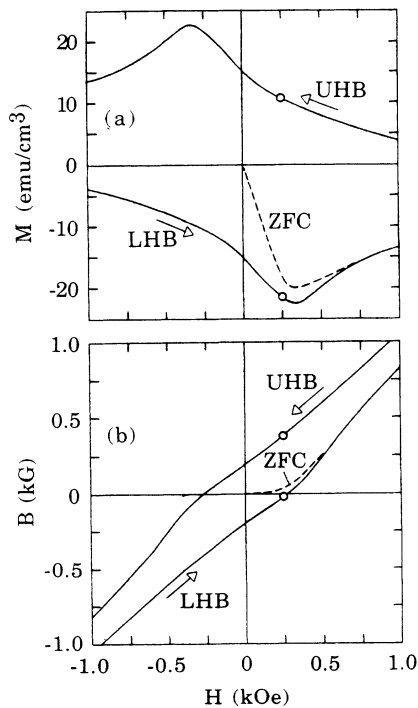


FIG. 1. (Ba,K)BiO<sub>3</sub> at 4.2 K. (a) Magnetization  $M$  and (b) flux density  $B$  versus field  $H$  for upper and lower hysteresis-loop branches (UHB and LHB) and for zero-field cooling (ZFC). Open circles represent UHB and LHB starting states for rotational measurements at  $H=0.25$  kOe (see Fig. 2).

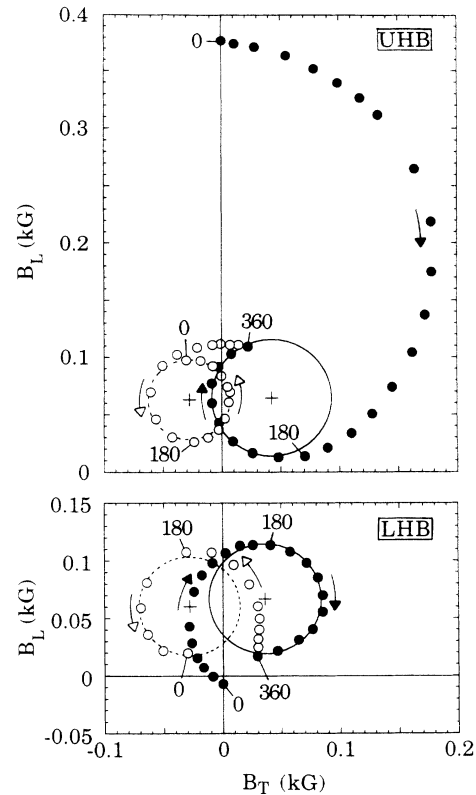


FIG. 2. (Ba,K)BiO<sub>3</sub> at 4.2 K. Polar plots of  $B_L$  versus  $B_T$  (longitudinal and transverse components of  $\mathbf{B}$  relative to  $\mathbf{H}$ ) for UHB and LHB starting states at  $H=0.25$  kOe. Closed and open circled points are for increasing and decreasing sample-rotation angle, respectively, labeled at intervals of  $180^\circ$ . Centers of fitted circles are indicated by + signs.

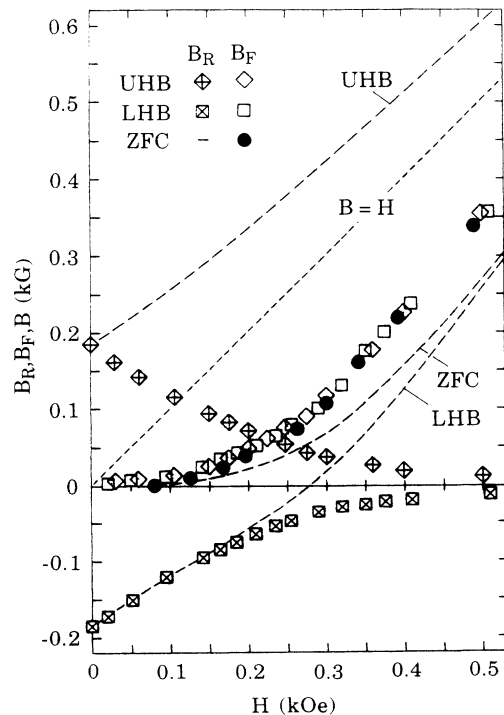


FIG. 3. (Ba,K)BiO<sub>3</sub> at 4.2 K. Rotational and frictional components of  $\mathbf{B}$  ( $B_R$  and  $B_F$ ) versus field  $H$  for UHB, LHB, and ZFC starting states (represented by dashed curves of  $B$  versus  $H$ ). Line for  $B=H$  is shown as short dashed.

The RMV measurements were repeated for UHB and LHB starting states at various fields between zero and 0.5 kOe, for which qualitatively similar polar plots of the  $\mathbf{B}$  vector were obtained. Our results for the  $B_R$  and  $B_F$  components are plotted versus  $H$  in Fig. 3. In both the UHB and LHB cases,  $B_R$  decreases in magnitude monotonically with increasing  $H$ , starting from the remanence values of opposite polarity at zero  $H$ . The absolute values of  $B_R$  in the two cases are essentially equal at all fields. Moreover, the close rotational similarity between the two cases also includes the values of  $B_F$ —which, in both cases, rise very slowly and then more rapidly with increasing  $H$ , lying consistently between the UHB and LHB starting-state curves (shown dashed in Fig. 3) and below the  $B = H$  line. Thus, despite the large differences between the starting states on the two branches of the major loop, the basic rotational properties represented by  $B_R$  and  $B_F$  are remarkably the same.

However, since  $B_R$  goes to the remanence value at zero  $H$ , the agreement between its values at various  $H$  pertains specifically to the two branches of the same hysteresis loop. This is borne out by our RMV measurements for starting states on the initial ZFC curve (shown dashed in Fig. 3), where we find that  $B_R$  is zero at all fields, even above  $H_{c1}$  ( $\sim 0.08$  kOe), which indicates that all the vortices produced by low fields after zero-field cooling are pinned rather weakly. Consequently, in this ZFC case, there is only a frictional component  $B_F$ , and this com-

ponent rises from zero at  $H_{c1}$  and rapidly joins up with the  $B_F$  values for the UHB and LHB cases at higher fields, as shown in Fig. 3. Thus, it is the magnitude of  $B_F$  that behaves almost universally for a variety of starting states at the same  $H$ . Indeed, the fact that  $B_F$  depends only on  $H$ , regardless of the magnetic history before rotation, indicates that in the rotational steady state the frictional component of the vortex-flux density equilibrates with the magnetic (and thermal) environment and, hence, is probably located in regions adjacent to the external surfaces of the sample.

Over the same range of fields at 4.2 K, the angle  $\theta_F$  between  $\mathbf{B}_F$  and  $\mathbf{H}$  is  $\sim 30^\circ$  at a broad maximum centered at  $\sim 0.25$  kOe and then descends to  $\sim 20^\circ$  at 0.5 kOe. Correspondingly, the frictional torque  $H\phi_0 \sin\theta_F$  on each vortex line (of quantized flux  $\phi_0$ ) continues to rise to a peak near 0.5 kOe before diminishing very slowly at higher fields. The field dependence of the frictional (vortex-pinning) torque, which has been an important consideration within the critical-state model,<sup>3</sup> is currently being investigated as a function of temperature in this and other superconducting materials.

We are grateful to J. W. Garland for his helpful suggestions and to D. G. Hinks for the well-prepared (Ba,K)BiO<sub>3</sub> sample material. This work has been supported in part by the National Science Foundation under Grants No. DMR-90-24416 and No. DMR-92-21901.

<sup>1</sup>C. P. Bean, Phys. Rev. Lett. **8**, 250 (1962); Rev. Mod. Phys. **36**, 31 (1964).

<sup>2</sup>P. W. Anderson, Phys. Rev. Lett. **9**, 309 (1962); P. W. Anderson and Y. B. Kim, Rev. Mod. Phys. **36**, 39 (1964).

<sup>3</sup>Y. B. Kim, C. F. Hempstead, and A. R. Strnad, Phys. Rev. Lett. **9**, 306 (1962); Phys. Rev. **129**, 528 (1963); Rev. Mod. Phys. **36**, 43 (1964).

<sup>4</sup>W. A. Fietz, M. R. Beasley, J. Silcox, and W. W. Webb, Phys. Rev. **136**, A335 (1964); Gang Xiao, F. H. Streitz, A. Gavrini, M. Z. Cieplak, J. Childress, Ming Lu, A. Zwicker, and C. L. Chien, Phys. Rev. B **36**, 2382 (1987); P. J. Kung, M. P. Maley, M. E. McHenry, J. O. Willis, J. Y. Coulter, M. Murakami, and S. Tanaka, *ibid.* **46**, 6427 (1992).

<sup>5</sup>A. C. Mota, A. Pollini, P. Visani, K. A. Müller, and J. G. Bednorz, Phys. Rev. B **36**, 4011 (1987); M. Tuominen, A. M. Goldman, and M. L. Mecartney, *ibid.* **37**, 548 (1988); Y.

Yeshurun and A. P. Malozemoff, Phys. Rev. Lett. **60**, 2202 (1988); I. A. Campbell, L. Fruchter, and R. Cabanel, *ibid.* **64**, 1561 (1990); Lu Zhang, J. Z. Liu, M. D. Lan, P. Klavins, and R. N. Shelton, Phys. Rev. B **44**, 10 190 (1991).

<sup>6</sup>Liwen Liu, J. S. Kouvel, and T. O. Brun, Phys. Rev. B **38**, 11 799 (1988); J. Appl. Phys. **67**, 4527 (1990).

<sup>7</sup>Liwen Liu, J. S. Kouvel, and T. O. Brun, Phys. Rev. B **43**, 7859 (1991).

<sup>8</sup>R. J. Cava, B. Batlogg, J. J. Krajewski, R. C. Farrow, L. W. Rupp, A. E. White, K. T. Short, W. F. Peck, and T. Y. Komatani, Nature **332**, 814 (1988); D. G. Hinks, B. Dabrowski, J. D. Jorgensen, A. W. Mitchell, D. R. Richards, S. Pie, and D. Shi, *ibid.* **333**, 836 (1988).

<sup>9</sup>J. S. Kouvel and H. P. Goeckner, Philos. Mag. B **65**, 1293 (1992); H. P. Goeckner and J. S. Kouvel, J. Appl. Phys. **73**, 5860 (1993).